Passivity-Based Control of Switched-Mode Power Supply for Audio Amplification Systems

T. R. Oliveira
Instituto Federal de Minas Gerais - IFMG
Automation - Campus Betim
Betim, MG - BRAZIL
E-mail: thiago.oliveira@ifmg.edu.br

P. F. Donoso-Garcia, S. I. Seleme Jr., L. M. F. Morais
Universidade Federal de Minas Gerais - UFMG
Department of Electronic Engineering
Belo Horizonte, MG - BRAZIL
E-mails: pedro@cpdee.ufmg.br, seleme@cpdee.ufmg.br, lenin@cpdee.ufmg.br

***Abstract*—The behavior of audio amplifiers imposes a severe load disturbance on power supplies used in amplification systems. Such disturbance can produce an elevation of the ripple magnitude at the voltage rails. Switched-mode power supplies can reduce the increase of the ripple amplitude by employing larger capacitor banks at its output, or using control strategies that decrease its output impedance. This paper proposes the application of a nonlinear passivity-based control technique to a switched-mode power supply, which allows the reduction of the ripple magnitude without the need for bulky reservoir capacitors.**

I. Introduction

The performance of an audio power amplification system can be widely affected by the behavior of its power supply unit. Voltage variations on the power supply voltage rails can increase the amplified audio signal distortion by voltage clamping or introduction of intermodulation components in the signal spectrum, which is commonly observed in amplifiers with weak PSRR. Therefore, suitable regulation and low ripple on the voltage rails are desirable in order to assure high audio quality at the amplifier output and guarantee its designed maximum output voltage and power ratings. Conventional unregulated power supplies, which are employed in the great majority of audio systems, try to provide such features by using large reservoir capacitors at its output (higher than 20,000μF) and bulky magnetic components [1]. However, this costly solution would nevertheless holds a weak load regulation and none line regulation.

A straightforward alternative for the unregulated power supplies would be the application of switched-mode regulated topologies, which allows minimization of regulation problems and increases the integration level of the power supply unit. In such topologies the ripple on the voltage rails is the object of main concern. The ripple magnitude is defined by the interaction of the output impedance of the power supply with the harmonic components inserted in the delivered current by the operation of the amplifier [2]. The output impedance should be thus sufficiently small to attenuate such components and so provide a low level ripple. This can be achieved basically by increasing the converter output capacity or by means of closed loop control [3], [4]. In this paper the minimization of the ripple on the voltage rails will be performed through the utilization of a nonlinear passivity-based control strategy, which has been successfully used in other power electronics applications such as PFC converters [5].

This paper is organized as follows: Section II presents the power supply load profile and shows an easy method for estimating the magnitude of the ripple in the voltage rails. Section III describes the topology of the considered power supply and presents the energy based modelling procedure for the converter. Section IV presents the passivity-based controller structure and discusses the expected closed loop performance of the switched-mode power supply. The obtained experimental results are pointed out in Section V. Finally, the work conclusions and latter discussions are presented in Section VI.

II. Power Supply Load Profile

The load seen by the power supply is dependent on the amplifier class of operation, the amplifier output load and the musical program. In this paper, a linear class AB power amplifier was considered as a model for the power supply development and evaluation.

Fig. 1 presents the operation stages of a class AB power amplifier. Observing the current path, one could define the instantaneous power delivered by the power supply to the amplifier as shown in (1).

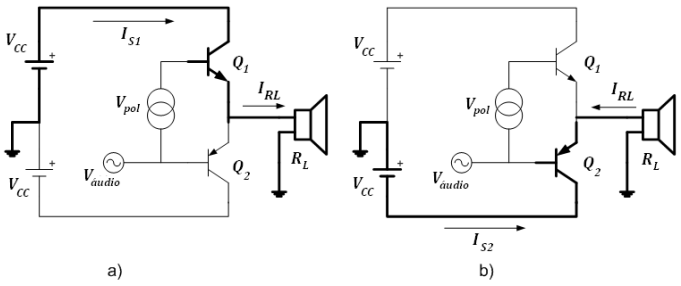

Fig. 1. Operation stages of a class AB power amplifier. a) Positive cycle of the output voltage. b) Negative cycle of the output voltage.

$$P_S(t) = V_{CC}(I_{S1} - I_{S2}) \tag{1}$$

Considering that the reference audio signal possess a sinusoidal profile, the waveform of the delivered power would be

similar to a full-wave rectified sinus, as shown in Fig. 2, with peak value as described in (2).

$$P_{Max} = V_{CC}\frac{V_{audio}}{R_L} \tag{2}$$

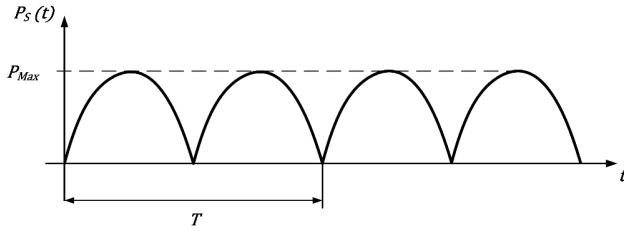

Fig. 2. Delivered power waveform.

Where:
V_{audio} - Peak voltage of the amplified audio signal.
T - Period of the audio signal.

Assuming that the voltage rails are regulated, *i.e*, V_{CC} is constant, the waveform presented at Fig. 2 would be identical to the one related to the delivered current. It becomes clear that the delivered current possesses a strong alternate behavior, which is determined by the amplifier output voltage and its load. The current can be decomposed in a Fourier series as displayed in (3).

$$i_S(t) = \frac{V_{audio}}{R_L}\left[\frac{2}{\pi} - \frac{4}{\pi}\sum_n \frac{1}{n^2-1}cos(n\omega_a t)\right] \qquad n = 2, 4, 6, 8... \tag{3}$$

Where:
n - Harmonic order.
ω_a - Audio reference angular frequency.

It can be seen that the frequency components within the delivered current spectrum are even harmonics of the amplified audio reference signal. The ripple magnitude can be estimated by the interaction of the current harmonic components with the power supply output impedance, as shown in (4).

$$\Delta V_{CC} = I_{Sn}Z_{out} \tag{4}$$

Where:
I_{Sn} - Amplitude of a n-order frequency component.
Z_{out} - Output impedance of the power supply.

Substituting I_{Sn} for the amplitude of the most significant harmonic component in the current spectrum (n = 2), one could determine the magnitude of the normalized ripple (*k*) as shown in (5).

$$k = \frac{4}{3\pi}\frac{V_{audio}}{V_{CC}}\frac{Z_{out}}{R_L} \tag{5}$$

The relation found in (5) is useful to estimate the performance of a power supply based on amplifier parameters and the power supply output impedance.

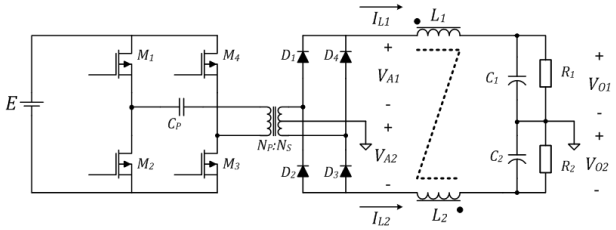

Fig. 3. Power stage structure of the audio power supply.

III. Switched-mode Power Supply

The configuration of the switched converter used in this work is presented in Fig. 3.

As seen in Fig. 3, the considered power supply topology is derived from a full bridge converter. The modified structure shows a mirrored output stage, which determines a dual voltage rail suitable to supply an audio power amplifier in single-ended configuration, and a coupled inductor at the output filter, which forces symmetry between the voltage rails during the system operation [3]. The parameters used in this converter are described in Table I.

TABLE I
Full bridge converter parameters

Parameter	Symbol	Value
Switching Frequency	F_S	96kHz
Voltage rail	V_{O1}; V_{O2}	35V
Minimum input voltage	E	153V
Transformer turn ratio	$\frac{N_P}{N_S}$	0.72
Blocking capacitor	C_P	10μF
Output filter inductor	L_1;L_2	185μH
Output filter capacitor	C_1;C_2	66μF
Equivalent output resistor	R_1;R_2	6.28Ω
Inductor magnetic coupling	k_{mag}	0.95

In order to synthesize a passivity-based control scheme for the full bridge converter it is interesting to perform the converter modelling based on the system energy relation characteristics [6]. For such purpose, the Euler-Lagrange modelling approach, discussed in [8], had shown to be a suitable solution. The Euler-Lagrange (EL) converter model can be constructed based on the EL equation presented in (6).

$$\frac{d}{dt}\left(\frac{\partial \ell}{\partial \dot{q}}\right) - \frac{\partial \ell}{\partial q} = \frac{\partial N}{\partial \dot{q}} + F_q \tag{6}$$

Where:
ℓ - Lagrangian;
q - Electrical charge;
$\dot{q}$ - Electrical current;
N - Rayleigh dissipation function;
F_q - External energy sources.

The Lagrangian is a term which represents the difference between the co-energy of the magnetic components ($M(\dot{q})$) and the electrical energy stored in the capacitors ($W(q)$), so that:

$$\ell = M(\dot{q}) - W(q) \tag{7}$$

The EL parameters, for the full bridge converter, are shown in (8) - (17), where the index '1' is used for the upper rail and '2' for the lower rail.

$$M_1(\dot{q_{L1}}) = \frac{1}{2}L_1\dot{q_{L1}}^2 + \frac{1}{2}L_M\dot{q_{L2}}^2 \tag{8}$$

$$M_2(\dot{q_{L2}}) = \frac{1}{2}L_2\dot{q_{L2}}^2 + \frac{1}{2}L_M\dot{q_{L1}}^2 \tag{9}$$

$$W_1(q_{C1}) = \frac{1}{2C_1}q_{C1}^2 \tag{10}$$

$$W_2(q_{C2}) = \frac{1}{2C_2}q_{C2}^2 \tag{11}$$

$$N_1 = \frac{1}{2}\left(\dot{q_{L1}} - \dot{q_{C1}}\right)^2 R_1 \tag{12}$$

$$N_2 = \frac{1}{2}\left(\dot{q_{L2}} - \dot{q_{C2}}\right)^2 R_2 \tag{13}$$

$$F_{qL1} = \mu V_{A1} \tag{14}$$

$$F_{qL2} = \mu V_{A2} \tag{15}$$

$$F_{qC1} = 0 \tag{16}$$

$$F_{qC2} = 0 \tag{17}$$

Where:
L_M - Mutual inductance at the coupled inductor;
μ - The switching command.
Assuming that:
$L = L_1 = L_2$
$C = C_1 = C_2$
$R = R_1 = R_2$
$\dot{q_L} = \frac{1}{2}\left(\dot{q_{L1}} + \dot{q_{L2}}\right)$
$q_C = q_{C1} + q_{C2}$
$V_A = V_{A1} + V_{A2}$
The solution of the EL equation can be written as:

$$\begin{cases} 2(L + L_M)\dfrac{d\dot{q_L}}{dt} = -2R(\dot{q_L} - \dot{q_C}) + \mu V_A \\ \frac{2}{C}q_C = 2R(\dot{q_L} - \dot{q_C}) \end{cases} \tag{18}$$

The relation found in (18) can be reformulated to be a function of the measurable states of the converter, such as the inductor current (i_L) and the output voltage (V_O). Assuming a variable change: $z_1 = i_L = \dot{q_L}$ and $z_2 = V_O = 2q_c/C$, the state equations for the converter can be written as:

$$\begin{cases} \dot{z_1} = -\frac{1}{2(L+L_M)}z_2 + \mu\frac{V_A}{2(L+L_M)} \\ \dot{z_2} = -\frac{2}{C}z_1 - \frac{1}{RC}z_2 \end{cases} \tag{19}$$

Or, in a matrix form, as:

$$D_B\dot{z} + (J_B + R_B)z = \mu E_B \tag{20}$$

Where:

$$z = \begin{bmatrix} z_1 \\ z_2 \end{bmatrix} \quad E_B = \begin{bmatrix} V_A \\ 0 \end{bmatrix} \quad J_B = \begin{bmatrix} 0 & 1 \\ -1 & 0 \end{bmatrix}$$

$$R_B = \begin{bmatrix} 0 & 0 \\ 0 & \frac{1}{2R} \end{bmatrix} \quad D_B = \begin{bmatrix} 2(L + L_M) & 0 \\ 0 & C/2 \end{bmatrix}$$

The model permits to define a storage function for the converter which measures the amount of energy stored in its passive elements. This function is shown in:

$$\mathcal{V}(z) = \frac{1}{2}z^T D_B z \tag{21}$$

IV. Passivity-based Controller

The passivity-based control is funded in energy concepts and consists in finding, for a given dynamical system, a control law with which the system stores less energy than the amount absorbed via the control action [6]. If the closed loop system fulfill the above requirement, it will provide asymptotic stability around an equilibrium point [7]. The passivity-based controller should then actuate in a way that the system closed loop dissipation function is enhanced in order to obtain a desired global storage function. Based on the converter storage function, shown in (21), a desirable closed loop storage function can be proposed as the one shown in (22).

$$\mathcal{V}_d = \frac{1}{2}\tilde{z}^T D_B \tilde{z} \tag{22}$$

By definition:

$$\tilde{z} \triangleq z - z_d \tag{23}$$

$$\tilde{z} = \begin{bmatrix} \tilde{z_1} & \tilde{z_2} \end{bmatrix}^T \tag{24}$$

$$z_d = \begin{bmatrix} z_{d1} & z_{d2} \end{bmatrix}^T \tag{25}$$

Where:
$\tilde{z}$ - Desired state error.
z_d - Desired state values.
z - Actual state values.
In order to enhance the dissipation structure of the closed loop system, the designed controller should insert a virtual damping term in the Rayleigh function of the system. The new dissipation function will then be presented as shown in (26).

$$N_d = \frac{1}{2}\tilde{z}^T R_{Bd}\tilde{z} = \frac{1}{2}\tilde{z}^T(R_B + R_{1B})\tilde{z} \tag{26}$$

Where:
R_{Bd} - Desired damping matrix.
R_{1B} - Inserted damping factor. $R_{1B} = \begin{bmatrix} R_1 & 0 \\ 0 & 0 \end{bmatrix}$.
The introduction of a virtual damping factor modifies the error dynamics of the converter, making the closed loop system more dissipative. The new error dynamics (Ψ) is shown in (27).

$$D_B\dot{\tilde{z}} + (J_B + R_{Bd})\tilde{z} = \Psi \tag{27}$$

Based on the definition for the error dynamics, a generic structure for the passivity-based controller can be proposed, such as the one shown in (28).

$$\Psi = \mu E_B - [D_B\dot{z_d} + (J_B + R_B)z_d - R_{1B}\tilde{z}] \tag{28}$$

System stability can be achieved by annulling the error dynamics. Assuming that the designed controller can perform such task, the controller structure will become as presented in (29).

$$\begin{cases} \dot{z_{d2}} = \frac{2}{C}(z_{d1} - \frac{1}{2R}z_{d2}) \\ \mu = \frac{1}{V_A}[2(L+L_M)\dot{z_{d1}} + z_{d2} - R_1(z_1 - z_{d1})] \end{cases} \quad (29)$$

The inserted damping factor (R_1) can be seen as a dissipative element in series with the equivalent inductance of the converter. Analyzing the controller equations, it becomes clear that the output voltage is controlled in a indirect manner, once the energy shaping is done by means of the inductor current state error, *i.e.*, the controller aims to regulate the inductor current and then the output voltage will be defined by the systems dynamic behavior. The inductor current reference (z_{d1}) is described in (30).

$$z_{d1} = \frac{1}{2R}V_{Od} + k_p(V_{Od} - z_2) + k_i\int_0^t [V_{Od} - z_2(\tau)]d\tau \quad (30)$$

Where:

V_{Od} - Desired output voltage.

k_p - Proportional gain.

k_i - Integral gain, used to prevent steady state errors.

The controller parameters used in this paper are specified in Table II.

TABLE II
PASSIVITY-BASED CONTROLLER PARAMETERS

Parameter	Value
V_{Od}	70V
R_1	22Ω
k_p	1
k_i	100

The performance of the power converter in amplification systems, as discussed in section II, can be estimated by its closed loop output impedance. Through simulation, the output impedance was obtained by the output voltage response of the converter to a load perturbation, which is characterized as an alternate current injected at the output end of the converter . The frequency response of the estimated output impedance is presented in the Fig. 4.

Through the output impedance found in Fig. 4 and the ripple definition, shown in (5), the maximum ripple can be estimated. Assuming, as an example, a 4Ω amplifier output load, a 35V voltage rail and a 26V amplified audio peak voltage, the maximum ripple expected would possess a 5.5% magnitude and occur in a 1.3kHz perturbation frequency. Unfortunately, the real ripple magnitude would be higher than the estimation due to voltage rails unbalance. The switching pattern cannot control the voltage rails in an independent manner, but only the difference between the two rails. This causes an energy exchange between them increasing the ripple observed on each rail. Such effect is minimized by the coupled inductor but not eliminated, meaning that a minimum ripple would always be present on the supplied voltages, specially in the low frequency range.

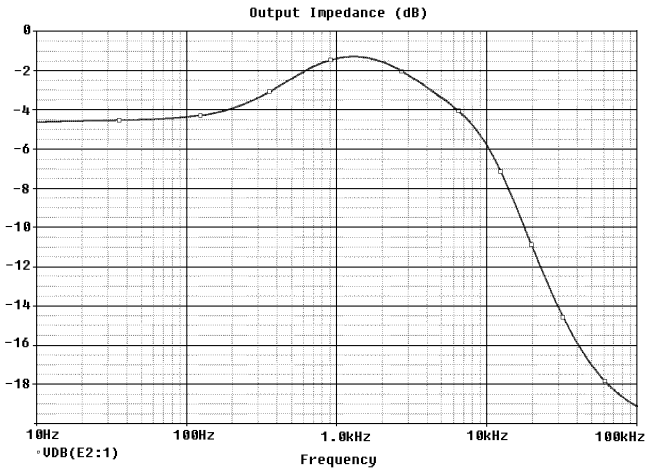

Fig. 4. Full bridge output impedance.

V. EXPERIMENTAL RESULTS

The power supply based on a full bridge converter was implemented and evaluated using the designed indirect passivity-based controller. A class AB audio power amplifier designed for high-end applications was used as the power supply load. The tests were conducted using an amplified audio voltage of $50V_{pp}$ and resistive loads of 5Ω and 8Ω plugged at the amplifier output. The passivity-based controller was implemented in an analog manner as shown in Fig. 5. The components values used in the controller are presented in Table III.

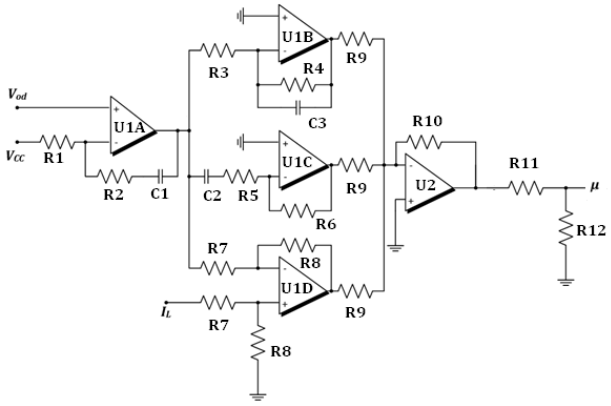

Fig. 5. Implemented passivity-based controller structure.

A. Passivity-based control evaluation

At a first moment, a frequency sweep of the audio reference signal was performed and the behavior of the ripple was then evaluated for different load values. The Fig. 6 presents the obtained curves. The ripple magnitude observed in the low frequency band presents a much higher value than estimated by the theoretical model. The variance occurs due to the voltage

TABLE III
PASSIVITY-BASED CONTROLLER COMPONENTS

Parameter	Value
U_1, U_2	LM6171
R_1	2.2kΩ
R_2, R_8	22kΩ
R_3, R_6, R_7, R_9	10kΩ
R_4, R_{11}, R_{12}	12kΩ
R_5	1.8kΩ
R_{10}	4.7kΩ
C_1	47nF
C_2	5.6nF
C_3	33nF

unbalance between the rails, which is more significant in lower frequencies. In spite of the mentioned discrepancy, the power supply shows an average ripple around 10% up to 900Hz and lower magnitudes in higher frequencies. Besides that, the variation of the amplifier load has a strong effect on the ripple magnitude, an 8Ω load induces a 33% magnitude reduction on the ripple obtained for a 5Ω load.

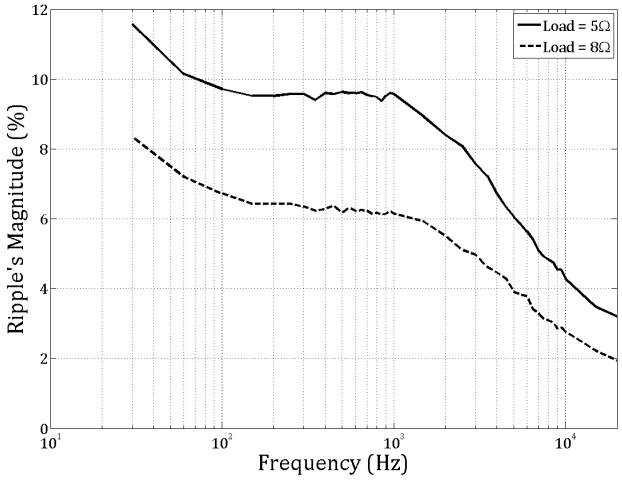

Fig. 6. Frequency sweep showing the ripple response of the positive rail of a passivity-based controlled power supply.

The ripple magnitude allows the amplified audio voltage to exhibit a high level amplitude (>70% of V_{CC}) without compromising the audio output quality. Fig. 7 shows the waveforms of the voltage rails and the audio amplified signal for a 250Hz audio frequency. It can be seen that the voltage undulations on the voltage rails did not cause clamping on the amplified signal, thus the obtained distortion was 1.4%, which is within the normal range for this power rating.

B. Comparison with linear controlled converter

In this item the achieved performance for the designed control strategy is compared with the one obtained for a conventional linear control system. For this experiment a linear control scheme was implemented considering a cascaded

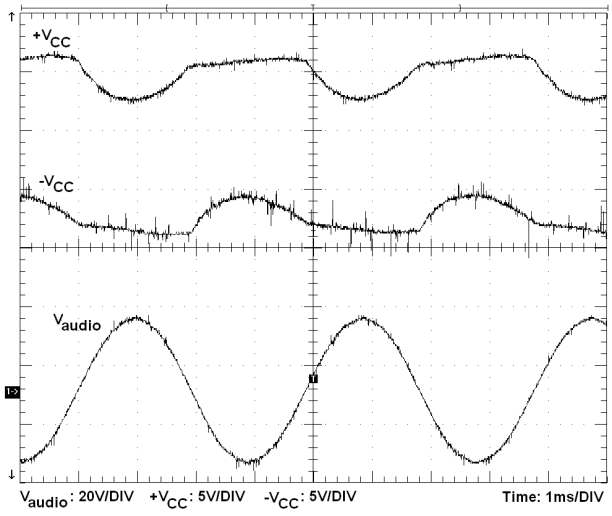

Fig. 7. Output Waveforms for a passivity-based controlled full bridge converter. Audio frequency = 250Hz and amplifier load = 5Ω.

structure, with a fast current loop and a slower voltage loop. The design of the compensators was accomplished through an optimized algorithm for buck-like converters proposed in [9]. This algorithm known as *factor-k approach* defines the parameters values for a determined compensator circuit so that the closed loop response of the converter fulfills requirements such as phase margin and crossover frequency. Considering a type II compensator structure and a 60° phase margin, new tests were performed with the full bridge converter. The results obtained by the frequency sweep of the audio signal are compared with the ones raised for the passivity-based control scheme and presented in Fig. 8.

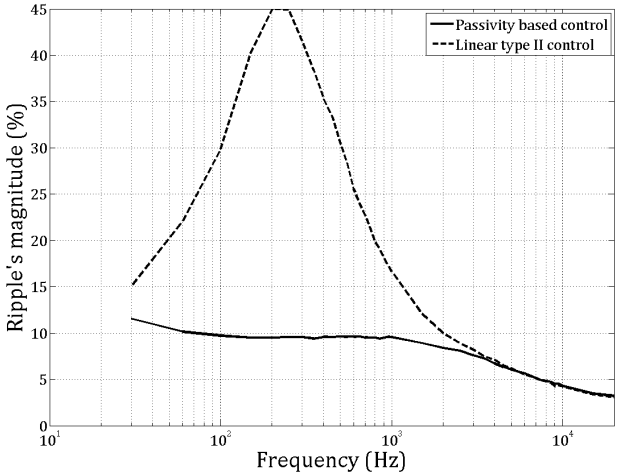

Fig. 8. Comparative analysis of a passivity-based and linear controlled power supply.

Fig. 8 shows that the linear control cannot achieve a suitable performance, since the obtained ripple magnitude is much higher than the one observed for the passivity-based system, reaching values beyond 40%, which can induce severe voltage

distortion at the amplified audio voltage. In order to improve the performance of the linear system, the capacity of the converter output filter could be increased. Fig. 9 shows the waveforms for the audio amplified signal and the voltage rails observed for the linear controlled system. As expected the ripple magnitude affects the audio amplified signal producing voltage clamping and raising the harmonic distortion, which reaches 7.5%.

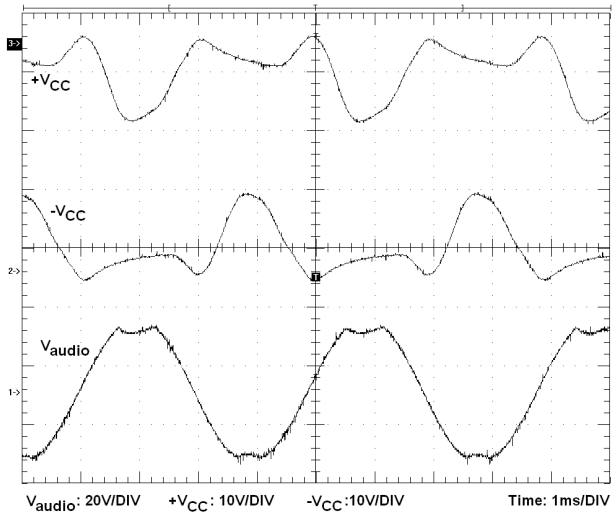

Fig. 9. Output Waveforms for a linear type II controlled full bridge converter. Audio frequency = 250Hz and amplifier load = 5Ω.

VI. Conclusion

This paper presented the evaluation of a passivity-based control strategy for a power supply unit, based on a full-bridge converter topology, used in audio amplification systems. It was shown that the ripple magnitude on the voltage rails can be estimated by means of the power supply output impedance and amplifier output parameters, such as rail voltage, output signal amplitude and amplifier load. However, due to voltage unbalance on the rails, produced by the converter incapacity for controlling each rail individually, the obtained ripple for low and middle frequency ranges have shown a higher magnitude than expected. Such contrast between the theoretical model and the real system can be reduced by employing a converter configuration which allows independent rail control. In spite of that, the experimental results have demonstrated that the application of passivity-based control can provide a suitable performance, in terms of ripple on the voltage rails ($\approx 10\%$), allowing the amplified audio signal to reach high amplitudes without clamping. Even though the converters output passive elements (inductor and capacitor) present low values, which hampers the control task, the passivity-based system achieved a good behavior.

The obtained performance was compared with a conventional linear control topology, designed by a standardized method. It was noticed that the linear system exhibits a much higher ripple than the passivity-based solution, reaching approximately 45% in its worst case. The larger ripple magnitude produced voltage clamping and high harmonic distortion, over 7.5%, which stays beyond the accepted levels for audio applications, while the passivity-based controlled system produced a THD of 1.4%.

The experimental results have shown that the passivity-based control technique can be employed to improve the performance of the power supply unit in audio systems, allowing the reduction of passive components without compromising the output audio quality. It was also shown that passivity-based control exhibits better performance than standard linear control with low output capacitor values.

Acknowledgment

The authors would like to thank FAPEMIG for supporting and funding the research project.

References

[1] E. Mendenhall, *Power supply regulation in audio power amplifiers*, 113th Audio Engineering Society Convention, conference paper nº 5694, 2002.

[2] L. Risbo and T. Morch, *Performance of an All digital power amplification system*, 104th Audio Engineering Society Convention, 1998.

[3] T. R. Oliveira, *Estudo e implementação de uma fonte chaveada empregando controle baseado em passividade, para alimentação de amplificadores de potência de áudio,* Master Thesis, PPGEE-UFMG, 2011.

[4] T. Ogawa; Y. Miyazawa; K. Higuchi; T. Kajikawa; A. Shimizu and O. Yoshizawa, *Compact audio power supply using approximate 2DOF robust digital control,* SICE annual conference, p.p. 2142–2145, Tokyo, Japan, 2008.

[5] E. A. Oliveira, *Aplicação do Controle Baseado Em Passividade Em Conversores Estáticos Operando Como Pré-reguladores de Fator de Potência,* Master Thesis, PPGEE-UFMG, 2008.

[6] E. A. Oliveira; L. M. F. Morais; S. I. Seleme Jr.; P. F. Donoso-Garcia; P. C. Cortizo and B. Cougo, *Power Factor Correction via Passivity-Based Adaptive Controller Using a Buck Converter Operating in Continuous Mode,* IEEE Workshop on Control and Modeling for Power Electronics (COMPEL 08), p.p. 1–6, 2008.

[7] R. Ortega; A. Loría; P. J. Nicklasson; and H. Sira-Ramírez, *Passivity-based control of euler-lagrange systems: Mechanical, electrical and electromechanical applications,*, Springer–Verlag, 1^{st} edition, London, England, 1998.

[8] H. Sira-Ramírez and M. D. de Nieto , *A Lagrangian Approach to Average Modelling of Pulsewidth-Modulation Controlled Dc-to-DC Power Converters,*, IEEE transactions on Circuits and Systems - Fundamental Theory and Applications, vol. 43, nº 5, p.p. 427–430, 1996.

[9] W. H. Lei and T. K. Man , *A General Approach for Optimizing Dynamic Response for Buck Converter,*, AND8143/D - ON Semiconductor, Application Note, Rev.0, 2004.